NAVAL POSTGRADUATE SCHOOL
Monterey, California

THESIS

ANALYSIS OF THE WATERHAMMER CONCEPT AS A MINE COUNTERMEASURE SYSTEM

by

Ronald J. Karun

September 2000

Thesis Advisor:	Andres Larraza
Second Reader:	John Pearson

Approved for public release; distribution is unlimited

REPORT DOCUMENTATION PAGE	*Form Approved* *OMB No. 0704-0188*

1. AGENCY USE ONLY *(Leave blank)*	2. REPORT DATE September 2000	3. REPORT TYPE AND DATES COVERED Master's Thesis	
4. TITLE AND SUBTITLE: Title (Mix case letters) Analysis of the Waterhammer Concept as a Mine Countermeasure System		5. FUNDING NUMBERS	
6. AUTHOR(S) : LT Ronald J. Karun			
7. PERFORMING ORGANIZATION NAME(S) AND ADDRESS(ES) Naval Postgraduate School Monterey, CA 93943-5000		8. PERFORMING ORGANIZATION REPORT NUMBER	
9. SPONSORING / MONITORING AGENCY NAME(S) AND ADDRESS(ES) N/A		10. SPONSORING / MONITORING AGENCY REPORT NUMBER	

11. SUPPLEMENTARY NOTES The views expressed in this thesis are those of the author and do not reflect the official policy or position of the Department of Defense or the U.S. Government.	
12a. DISTRIBUTION / AVAILABILITY STATEMENT Approved for public release: distribution is unlimited	12b. DISTRIBUTION CODE

13. ABSTRACT *(maximum 200 words)*

The purpose of this thesis is to provide an analysis of the Waterhammer concept design. Waterhammer is a device intended to generate repetitive shock waves to clear a path through the very shallow water region for amphibious operations. These repetitive shock waves are intended to destroy obstructions and mines alike.

This thesis analyzes the energy budget of the deflagration processes and the basic principles of shock waves and acoustic saturation When the source amplitude is increased to very high levels, acoustic saturation sets in, a state in which the amplitude of the received signal approaches a limiting value, independent of the source amplitude. Acoustic saturation thus will set physical constraints in the design of Waterhammer. Furthermore, as the pulse propagates in the shallow water environment, reflections from the water's surface and bottom floor will spread the energy in the water column thus reducing the energy density These combined effects can affect the intended performance of Waterhammer. The results of the analysis in this thesis lead to the conclusion that Waterhammer may not be viable in its present concept design..

14. SUBJECT TERMS Waterhammer performance. Acoustic Saturation Limits. Nonlinear effect in water due to very high source levels	15. NUMBER OF PAGES 68
	16. PRICE CODE

17. SECURITY CLASSIFICATION OF REPORT Unclassified	18. SECURITY CLASSIFICATION OF THIS PAGE Unclassified	19. SECURITY CLASSIFICATION OF ABSTRACT Unclassified	20. LIMITATION OF ABSTRACT UL

THIS PAGE INTENTIONALLY LEFT BLANK

ANALYSIS OF THE WATERHAMMER CONCEPT AS A MINE
COUNTERMEASURE SYSTEM

Ronald J. Karun
Lieutenant, United States Navy
B.S., United States Naval Academy, 1993

Submitted in partial fulfillment of the
requirements for the degree of

MASTER OF SCIENCE IN ENGINEERING ACOUSTICS

from the

NAVAL POSTGRADUATE SCHOOL
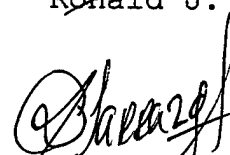September 2000

Author: _____
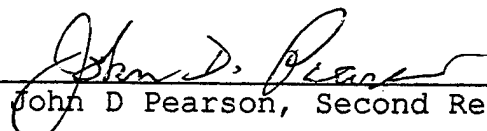Ronald J. Karun

Approved by: _____
Andres Larraza, Thesis Advisor

_____
John D Pearson, Second Reader

_____
Kevin Smith, Chairman, Engineering
Acoustics Academic Committee

iii

THIS PAGE INTENTIONALLY LEFT BLANK

ABSTRACT

The purpose of this thesis is to provide an analysis of the Waterhammer concept design. Waterhammer is a device intended to generate repetitive shock waves to clear a path through the very shallow water region for amphibious operations. These repetitive shock waves are intended to destroy obstructions and mines alike.

This thesis analyzes the energy budget of the deflagration processes and the basic principles of shock waves and acoustic saturation. When the source amplitude is increased to very high levels, acoustic saturation sets in, a state in which the amplitude of the received signal approaches a limiting value, independent of the source amplitude. Acoustic saturation thus will set physical constraints in the design of Waterhammer. Furthermore, as the pulse propagates in the shallow water environment, reflections from the water's surface and bottom floor will spread the energy in the water column thus reducing the energy density. These combined effects can affect the intended performance of Waterhammer. The results of the analysis in this thesis lead to the conclusion that Waterhammer may not be viable in its present concept design.

THIS PAGE INTENTIONALLY LEFT BLANK

TABLE OF CONTENTS

THIS PAGE INTENTIONALLY LEFT BLANK

LIST OF FIGURES

THIS PAGE INTENTIONALLY LEFT BLANK

EXECUTIVE SUMMARY

The purpose of this thesis is to provide an analysis of the Waterhammer concept design. Waterhammer is a device intended to generate repetitive shock waves to clear a path through the very shallow water region for amphibious operations. These repetitive shock waves are intended to destroy obstructions and mines alike.

This thesis analyzes the energy budget of the deflagration processes and the basic principles of shock waves and acoustic saturation. When the source amplitude is increased to very high levels, acoustic saturation sets in, a state in which the amplitude of the received signal approaches a limiting value, independent of the source amplitude. Acoustic saturation thus will set physical constraints in the design of Waterhammer. Furthermore, as the pulse propagates in the shallow water environment, reflections from the water's surface and bottom floor will spread the energy in the water column thus reducing the energy density. These combined effects can affect the intended performance of Waterhammer. The results of the analysis in this thesis lead to the conclusion that Waterhammer may not be viable in its present concept design.

THIS PAGE INTENTIONALLY LEFT BLANK

ACKNOWLEDGMENTS

THIS PAGE INTENTIONALLY LEFT BLANK

I. INTRODUCTION

A. BACKGROUND

Mine Warfare (MIW) was born into existence in 1777 through the efforts of David Bushnell. Bushnell designed the first sea mine, a floating keg containing black powder and a rudimentary contact trigger. Robert Fulton continued on with this research and subsequently designed several other mines between 1797 and 1812. For many years after their first use "… the sea mine was considered a 'devilish device' used only by the 'unchivalrous' nations" (Ref. 1). Because of this rational, Fulton was unable to sell his mine designs to various countries, despite being successfully tested.

It was not until the American Civil War before the true practicality and potential of the sea mine became known. During this war, the inferior Confederate Navy compensated for their insufficiency with sea mines. The cheap and quickly produced sea mines used by the Confederates sunk twenty seven Federal ships, while artillery only sunk nine ships. Despite a respectable showing, mines had not become an accepted and significant force in naval war strategy until World War I.

1

During World War I, mines became the primary weapon against German Submarines. A barrier of sea mines was placed between Scotland and Norway (250 miles) in an attempt to contain German U-boats. Although the barrier was not completed prior to the end of the war, 72,000 mines were seeded in the five months prior. This minefield sank at least six submarines and damaged many more. Soon after the war, sea mines were once again forgotten. The passive, unspectacular nature of the sea mine causes many nations to lose interest in the sea mine during times of peace. But during times of conflict, low costs, quick production times, and effectiveness attract these same nations.

Not until 1967, during the Vietnam Conflict, did the initial "bomb-type" sea mine appear. These mines, known as "destructors", were the first to contain sophisticated firing mechanisms. They activated by magnetic or seismic activity instead of contact, bringing the sea mine to a whole new level of complexity, effectiveness and practicality. Since 1967, mines have continued to evolve, becoming more complicated, while still maintaining their relatively low production costs.

B. SETBACK

Although mines have continued to grow in popularity and complexity, the methods for finding and disposing of them has ceased to evolve. Currently, third world countries can significantly delay or prevent amphibious operations along their coastline by seeding simple, World War I era mines.

The United States Military is unable to quickly and effectively clear a path to the beach through hostile, mined waters. The area that provides the most significant problem lies within the surf zone (10-40 feet). The only methods of clearing this region are the use of Explosive Ordinance Disposal Teams (EOD), Marine Mammals, and Special Forces. These forces first must conduct a survey of the area identifying mine-like contacts. Then each contact must be re-acquired and identified. Finally the contacts identified as mines will be neutralized. These tactics place highly trained U.S. forces in the line of fire, while they meticulously perform a slow, methodical mission. This also foreshadows the possibility of an impending amphibious assault, allowing the enemy the time to reinforce their positions and prepare for the assault. The development of

a new method or device for mine clearance is essential to the survival of amphibious operations, as we know them.

C.   A PROPOSED SOLUTION

A concept solution, called Waterhammer has been proposed. In its present concept, Waterhammer is an Unmanned-Underwater Vehicle (UUV) intended to neutralize mines and destroy obstacles by delivering a bombardment of high-pressure impulses, providing a clear path to the beach for future amphibious operations. These high-pressure impulses, or shock waves would be the result of a deflagration of an aluminum powder fuel contained within the device. If this concept can be realized, it would simplify the mine clearance tactics by eliminating the requirements for survey, identification and neutralization operations. Furthermore, it would complete its mission without jeopardizing U.S. forces.

It is the purpose of this thesis is to provide a critical analysis of the Waterhammer concept design. In Chapter II an analysis of the energy budget of deflagration processes is made, in particular, the amount of acoustic energy liberated by the reaction. Chapters III and IV deal with basic principles of shock waves and acoustic saturation, respectively. In particular, Chapter IV

emphasizes the notion that there is a limit to the maximum amount of input (chemical) energy that can be converted to acoustic energy. When the source amplitude is increased to very high levels, acoustic saturation sets in, a state in which the amplitude of the received signal approaches a limiting value, independent of the source amplitude. Acoustic saturation thus will set physical constraints in the design of Waterhammer. As the pulse propagates in the shallow water environment, reflections from the surface of the water and the bottom floor will spread the energy of the initial pulse over the water column. Furthermore, bottom absorption will also remove acoustic energy. These combined effects will affect the intended performance of Waterhammer. Chapter V illustrates the physical descriptions and conditions of the apparatus and test site. In Chapters VI, a simulation of the multi-path propagation is presented and compared with the results of a field test in Aberdeen Proving Grounds, MD. The results of the analysis in this thesis lead to the conclusion that Waterhammer may not be viable in its present concept design.

THIS PAGE INTENTIONALLY LEFT BLANK

II. DEFLAGRATIONS

A. OVERVIEW

When an explosion is initiated within a mass of
explosive material, a pressure wave is formed within that
material. It is then transmitted into the surrounding
medium. This pressure wave is caused by a complex series
of phenomena during the conversion of the explosive
material into gaseous reaction products. The speed at
which the pressure wave propagates through the material and
the rate at which the reaction takes place is dependant
upon the type of explosive material used. In "high"
explosives like TNT, the velocity of detonation is between
15,000 and 30,000 ft/s, whereas materials such as black
powder produce velocities of only .1 to 1 ft/s. This speed
is the basis for categorizing the explosive process.
Detonations, such as with TNT, are supersonic reactions,
while the chemical reaction found in black powder, is
called deflagration. The speed of deflagrations is
contained solely in the subsonic region. These speeds also
create two vastly different pressure pulses, as Figure 2.1
illustrates. The detonation material, TNT, creates a shock
wave characterized by an infinitely steep front, a high
peak pressure, and a rapid decay. The deflagrating
material, black powder, generates a relatively low, broad

7

pressure pulse. The width of the corresponding pressure pulse is determined by the rate at which the material consumes itself.
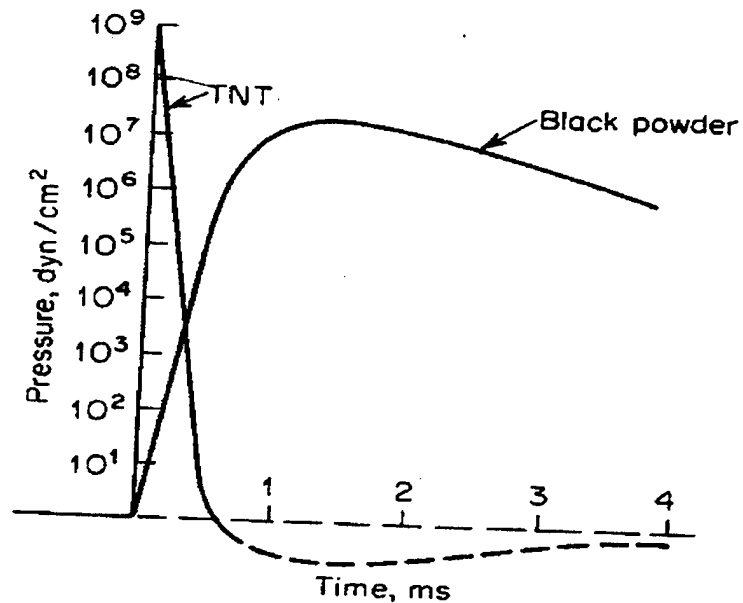
Figure 2.1 - Pressure as a function of time for a deflagration of black powder compared to a comparable detonation of TNT (Ref. 2).

B.   BURN RATE

In a deflagration the chemical reaction that takes place is through a rapid progressive burning of the exposed, unburned surface of the explosive material. The size and shape of the grains within the explosive control the rate of the chemical reaction, while the amount of exposed, unburned area dictates the burn rate. As the chemical reaction proceeds, the surface of the burning

8

explosive recedes layer by layer in a direction normal to the surface until the complete particle or grain is consumed. This rate of regression, or linear burn rate, designated r, can be calculated with Vieille's Law (1893).

$$r = \beta \, P^{\alpha} \qquad \text{(Eqn. 2.1)}$$

The index α, known as the burning rate index, has to be determined experimentally. Typical values for α are between 0.3 and 1.0. The coefficient of burning rate is β, and P is the pressure resident at the surface of the explosive. As the burn rate increases, the period of the corresponding pressure pulse decreases accordingly. Using this knowledge, Waterhammer uses an aluminum powder based fuel.

C. DESTRUCTIVE PROPERTIES

For underwater operations, a shock wave of significant period must be generated to create the destructive power required to neutralize mines and obstructions. Since bottom mines are not rigidly affixed to the bottom and moored mines are free to float within the water column, a short pressure impulse will simply move the mine or obstruction off to the side instead of rendering it useless. In order to obtain the maximum destructive force,

the intended object must be completely enveloped within the pressure pulse. By completely enveloping the target with the pressure pulse, the target does not get simply pushed aside (pressure on each side is equal) and a maximum destructive force may be achieved. With the high-pressure shock wave completely encapsulating the target, the shock pressure may stress the target beyond its elastic limit causing permanent deformation or rupturing the hull of the mine. In principle, through continuous bombardment, mines can be rendered useless and obstructions can be destroyed. For most mines, a 450 μs pulse is required to envelop the typical obstruction or mine cross section. This 450 μs pulse moving at the nominal sound speed in water of 1500 m/s envelops a length of .675 m or 2.21 ft.

D. FUEL SELECTION AND MIXING

In the concept design for Waterhammer to be effective, the explosive fuel must have the following characteristics. First, the explosives must create a long pressure pulse, so materials resulting in deflagrations are the obvious choice. The fuel must also possess the required burn rate to be able to produce the proper period and high pressures required to effectively neutralize the target. Waterhammer is designed to use 40 g of fuel within each combustion

10

chamber. Using Eqn. 2.1 with an intended fuel load of 40 g (.04 kg) and a required period of 450 μs, a burning rate of 88.89 kg/s is required to form the desired pulse length. Vieille's Law for a required burn rate of 88.89 kg/s at a hydrostatic pressure of 2.24×10^5 Pa, which corresponds to a 40 ft depth, is satisfied by the α and β parameters for aluminum powder based fuel. This fuel source is inert until it is mixed with water, which will be provided by the sea. Even when it is mixed, in proper proportions, with water, the shock from a spark discharge must be applied to trigger the reaction. This allows the device to be transported safely or even refueled without the worry of accidental combustion.

In any combustion, the ratio of available fuel to oxidation agents is the fundamental method for determining the perfect, stoichiometric, mix. In the case of Waterhammer, aluminum powder is mixed with water in the following proportions:

$$\textbf{2 Al + 3 H}_2\textbf{O} \rightarrow \textbf{Al}_2\textbf{O}_3 \textbf{ + 3 H}_2 \textbf{ + 820 kj}$$
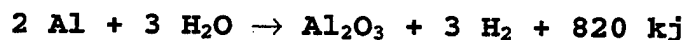
The reaction yields 820 kj of energy released by 108 g of fuel, or roughly 7.6 kj for every gram of fuel. This energy is then transformed into heat, light and pressure.

11

Although this is the intended fuel, alternative fuels have been used during testing. These alternate fuels substitute Hydrogen Peroxide for water, yielding the following reactions:

$$2\ Al\ +\ 3\ H_2O_2\ \rightarrow\ Al_2O_3\ +\ 3\ H_2O\ +\ 1960\ kj$$

$$4\ Al\ +\ 3\ H_2O_2\ \rightarrow\ 2\ Al_2O_3\ +\ 3\ H_2\ +\ 2780\ kj$$
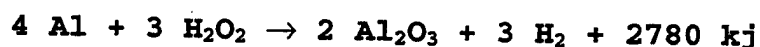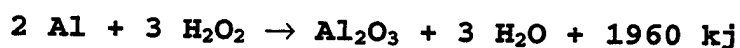
These reactions yield 12.56 kj/g and 13.24 kj/g respectively. This allows more energy to be produced in each reaction, creating higher pressures with less fuel. Since hydrogen peroxide is relatively inexpensive, using the aluminum peroxide mix allows one to use less fuel in each shot to generate the same pressures and energy generated by the aluminum water mixture. Although the aluminum peroxide mix produces more energy per gram of fuel it will not be used in a final product for three main reasons. First and foremost is safety, in this form a large spark would ignite the mixture causing a premature deflagration. Second, the aluminum peroxide solution decomposes rapidly thus limiting the storage capability of the fuel. Finally, an aluminum peroxide fuel takes up significantly more space than just aluminum powder. The fuel storage capacity of this device is limited, so by

using the surrounding saltwater as a reactant serves to conserve fuel storage space.

Once the proper proportions of aluminum and water/peroxide are combined and present within the combustion chamber, a spark initiates the deflagration. This subsonic reaction gradually builds up pressure and temperature within the combustion chamber, forming a high-pressure pulse, or shock wave, of the required period.

THIS PAGE INTENTIONALLY LEFT BLANK

III. SHOCK WAVES

A. OVERVIEW

A shock wave is a discontinuity of pressure moving through a medium. However, mass, momentum and energy are conserved across the shock front as it propagates through the medium. These conservation laws lead to three equations known as the *Rankine-Hugoniot Jump Equations*, which are used to describe the motion of the particles within the shock wave (Ref. 3).

Conservation of Mass:

$$\rho_1/\rho_0 = (U-u_0)/(U-u_1)$$

Conservation of Momentum:

$$P_1-P_0 = \rho_0(u_1-u_0)(U-u_0)$$

Conservation of Energy:

$$e_1-e_0 = [(P_1u_1-P_0u_0)/\rho_0(U-u_0)]-[(u_1^2-u_0^2)/2]$$

Shock Pressure is denoted by P (Gpa), while U is the shock velocity (km/s), u is particle velocity (km/s), ρ is density (g/cm^3) and e is the internal energy. The subscripts 0 and 1, refer to the state of the material before and after the shock, respectively. When the material is at rest, prior to the arrival of the shock, then u_0 can be neglected.

15

As the shock front propagates through a medium, the medium becomes compressed, increasing the density. This increase in density causes the remaining portion of the shock wave to increase in velocity. Therefore the particles just behind the shock front push against the particles at the shock front and further push the wave along. Simply, the shock velocity is greater than the sound velocity in the unshocked material. The particle velocity is expressed through the empirical relationship called the velocity Hugoniot equation (Ref. 3):

$$U = c_0 + su$$

Where c_0 is the bulk sound speed and s is the velocity coefficient. The values of c_0 and s are determined experimentally for various materials.

As shock waves travel through the medium they attenuate, although the attenuation process is slightly different than that of a sound wave. The shock wave not only loses energy due to thermo-viscous dissipation as it travels through a medium, but it also loses amplitude due to its interaction with a rarefaction wave. Using Waterhammer as an example, where a relatively square-wave pulse is generated through a deflagration. The front of the shock wave is traveling at velocity U, which is

determined by P and ρ_0. The shock front then compresses the
medium and a corresponding rarefaction wave begins
traveling at velocity, R, determined by the quantities, ρ, P
and u of the material behind and in front of it. R, which
is traveling into a material at density ρ_1, is greater than
U, which is traveling into a material of density ρ_0
(unshocked). Simply, the rarefaction wave velocity R is
greater than the shock wave velocity U and can be expressed
as follows (Ref. 3):

$$R = c_0 + 2su$$

The Rarefaction wave then progresses into the square
region, where the shock wave shape changes from a square-
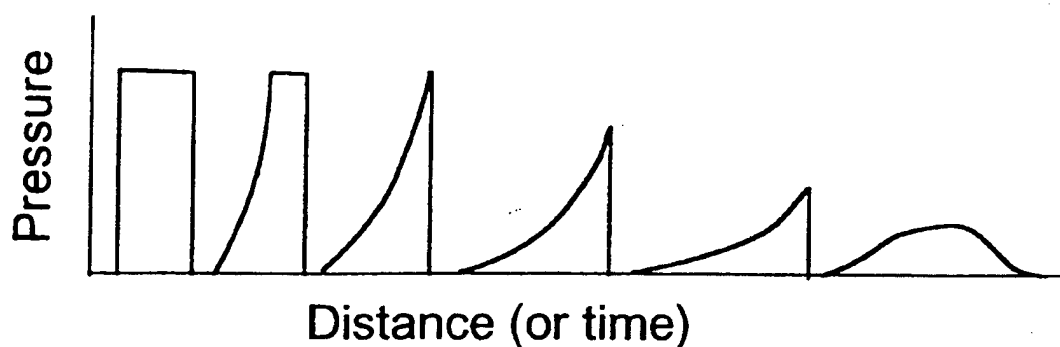wave to form a shape resembling a sawtooth, as Figure 3.1
illustrates.

Figure 3.1 - Progression from a square wave through
maturity (sawtooth region) and into "old age" (sinusoidal
shape) (Ref. 3).

17

The interaction with the rarefaction wave causes a peak pressure drop across the wave front. As the peak pressure in the front of the shock drops, so does the shock velocity U. As the wave propagates further in range, this process continually repeats until the peak pressure drops to such a low value that the shock wave becomes a sound wave. These effects can be expressed in terms of a distortion range variable, σ. This variable is defined as (Ref. 4):

$$\sigma = \beta \varepsilon k r_0 \ln(r/r_0)$$

where

$$\varepsilon = P_0/\rho_0 c_0^2.$$

The shock first forms at range, $\Re$, when $\sigma = 1$. At range, r, the saw tooth becomes fully formed and $\sigma = 3$. Within the saw tooth region rapid attenuation is a result of nonlinear effects. They cause energy to be fed into the shocks where it is efficiently dissipated. But as the shocks weaken, they disperse and the shock dissipation is again slowed. Eventually ordinary small signal attenuation, which has been ignored up to this point, becomes more important than the attenuation associated with nonlinear effects. When this happens the wave reaches old

18

age and the waveform resembles a sinusoid. At this point the nonlinearity is of little consequence. The beginning of the old age region occurs at range, r_{max}. This is calculated as the range at which the rate of attenuation due to linear effects is equal to those of nonlinear effects. Expressions for the three ranges are as follows (Ref. 5):

$$\Re = r0 \; \exp(1/\beta\epsilon kr_0) \qquad \text{(Eqn. 3.1)}$$

$$r = r0 \; \exp(3/\beta\epsilon kr_0) = r_0(\Re/r_0)^3 \qquad \text{(Eqn. 3.2)}$$

$$r_{max} = \frac{\beta\epsilon kr_0/\alpha}{1+\beta\epsilon kr_0\ln(r_{max}/r_0)} \qquad \text{(Eqn. 3.3)}$$

Here, α is the appropriate small signal attenuation coefficient for the medium at the frequency, ω. Constant, β, depends upon the equation of state of the medium. For a gas it is given by $\beta = (1+\gamma)/2$, where γ represents the ratio of specific heats of the medium. Thus, for gases, $\beta = 1.2$. On the other hand for water, $\beta = 3.5$. The wave number, k, is $k = \omega/c$.

Since the terms ϵ and k appear together in each equation, the nonlinear effects increase with frequency and source level.

19

THIS PAGE INTENTIONALLY LEFT BLANK

IV. SATURATION

A. OVERVIEW

At low acoustic levels, the amplitude of a received signal at a fixed distance is directly proportional to the amplitude at the source. As the amplitude at the source is increased, the amplitude at the receiver does not increase in direct proportion indefinitely. When the source amplitude is increased to very high levels, acoustic saturation sets in, a state in which the amplitude of the received signal approaches a limiting value, independent of the source amplitude.

The nonlinear effect of acoustic saturation is rather a dependence of propagation velocity on the pressure amplitude of the sound wave. As discussed previously, high positive or negative pressures travel faster than slower ones causing the leading edge of the shock wave to progressively increase as it propagates, to eventually acquire a saw tooth waveform. As the waveform transforms into a saw tooth, harmonics of the fundamental frequency are generated. The harmonics are generated at the expense of the energy in the fundamental frequency. A portion of the power in the fundamental is converted into harmonics, where it is more rapidly lost because of the greater

21

absorption at higher frequencies. This harmonic conversion process is greater at higher amplitudes than at low ones so that, as the source level increases, the harmonic content increases as well. This brings rise to a saturation effect, whereby an increase of source level does not result in a proportional increase in the level of the fundamental frequency. However, spreading lessens the deleterious effects of harmonic conversion, by reducing the intensity of the primary wave. This delays the saturation effect of the fundamental in range.

Yet at any given range from a source, there must exist a maximum acoustic level, which the source can produce at a particular frequency. Thus, all additional energy pumped into the wave by the source is lost at the shock fronts, and acoustic saturation is said to have occurred.

Theoretical analyses of saturation have largely been based on Burgers' equation and on weak-shock theory. The solution of Burgers' equation shows that as particle velocity, u_0, becomes very large, the amplitude of the acoustic signal at a distant point, x, becomes independent of u_0. In particular, the saturation amplitude of the fundamental component u_1 is given by (Ref. 5)

$$U_{sat} = (4\alpha c_0/\beta k)e^{-\alpha x} \qquad \text{(Eqn. 4.1)}$$

where α is the small signal attenuation coefficient. Whitham's solution (1952) of the periodic radiation problem by means of weak shock theory leads to a different saturation amplitude,

$$U_{sat} = 2c_0/\beta kx \qquad \text{(Eqn. 4.2)}$$

This discrepancy is only apparent, since Witham's solution is valid only in the saw tooth region. Burgers' solution is valid in the more remote, old age region, where the shock waves have deteriorated and the waveform resembles a sinusoid. Laird (1955) expanded upon the previous equations to find the acoustic pressure saturation limit within the saw tooth region, where r is the radial distance from a source whose radius is r_0.

$$P_{sat} \text{ (sawtooth)} = 2\rho_0 c_0^2/\beta kr \ln(r/r_0) \qquad \text{(Eqn. 4.3)}$$

These saturation formulas are used to determine curves of maximum acoustic pressure, as a function of range, with frequency as a parameter. Once graphed, they show that once in a stable saw tooth waveform, $\sigma = 3$, energy in the wave is continually dissipated at the shock fronts, causing the amplitude of the pressure wave to decrease. The irreversible energy loss at shock fronts imposes an upper limit on how much sound power can be transmitted beyond

certain range. As the sources amplitude or frequency is increased, the shock formation moves closer to the source, with the subsequent increase of energy dissipated before the waves arrive at the observation point. Eventually, the amplitude is sufficiently reduced that nonlinear effects can no longer maintain a shock against thermal and viscous losses. All additional energy pumped into the wave by the source is lost at the shock fronts, and acoustic saturation has occurred. Thus, large amounts of power are wasted due to underestimating nonlinear effects.

V. APPARATUS AND TEST CONFIGURATION

A. OVERVIEW

Although the final product is far from completion and many more ideas are yet to be incorporated, the basic construction and design of Waterhammer has remained unchanged. It consists of a series of combustion chambers, attached to nozzles, which extend into the surrounding medium.

The combustion chamber is the singularly most important area within the device. Within this area, the aluminum powder is injected into the already present seawater creating a fuel slurry. Once this fuel slurry is produced, a large amplitude spark is applied and a deflagration results. As the deflagration burns, the high-pressure wave carries unburned fuel, waste products and gases through the nozzle and into the surrounding medium.

B. TEST APPARATUS

Testing of the product was conducted in three phases. The first phase consisted of a single nozzle used to establish a fuel mixture, fuel consistency, and isolate the pressure effects in each nozzle. The subsequent phase consisted of a 1 x 4 array designed to measure a relatively small pressure pulse of the correct width and amplitude.

25

These initial two phases were conducted in Alexandria, VA at the APTI (designers of the Waterhammer concept) laboratory. The final phase consisted of a 4 x 4 array tested at Aberdeen Proving Grounds in Aberdeen, MD. The purpose of this last phase was to estimate propagation losses and beam widths associated with the device.

During the initial testing phase, a combustion chamber and nozzle were used to demonstrate and test various fuel mixtures and the resulting combustion chamber pressures. In this structure, the measured pressures would be vastly different from expectations from a final product due to energy release to the adjacent water columns. In order to simulate the pressure field generated by other nozzles, an extender tube was placed on the end of the nozzle. This tube prevents excess energy from being dissipated into the immediate, surrounding water, which would be pressurized by the deflagrations within neighboring nozzles. The apparatus in Figure 5.1 illustrates the combustion chamber, nozzle assembly and extender tube. For the testing process, this device was inserted into a metal cylinder containing fresh water. Pressure sensors were then inserted in the combustion chamber, nozzle assembly and the base of the extender tube, as displayed in Figure 5.2.
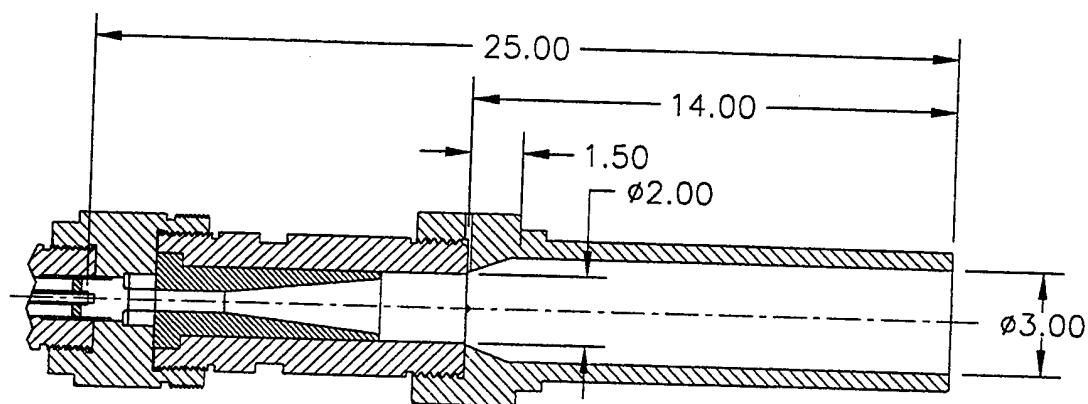
26

Figure 5.1 – Schematic of a single nozzle with a 14 inch extender tube applied.

During phase two, four nozzles and their independent combustion chambers were combined to form a linear array. In this series of experiments, the extender tubes were omitted since the multiple nozzles pressurized the surrounding medium. Four pressure sensors were placed at a height of 12 inches above each nozzle. An additional pressure sensor was placed within one of the four combustion chambers.

For the third and final phase, a four by four array was established, as seen in Figure 5.3, to model the associated beam width. This apparatus differs from previous renditions by attaching two nozzles to each combustion chamber, resulting in 32 nozzles attached to 16 combustion chambers. In order to develop a recoilless
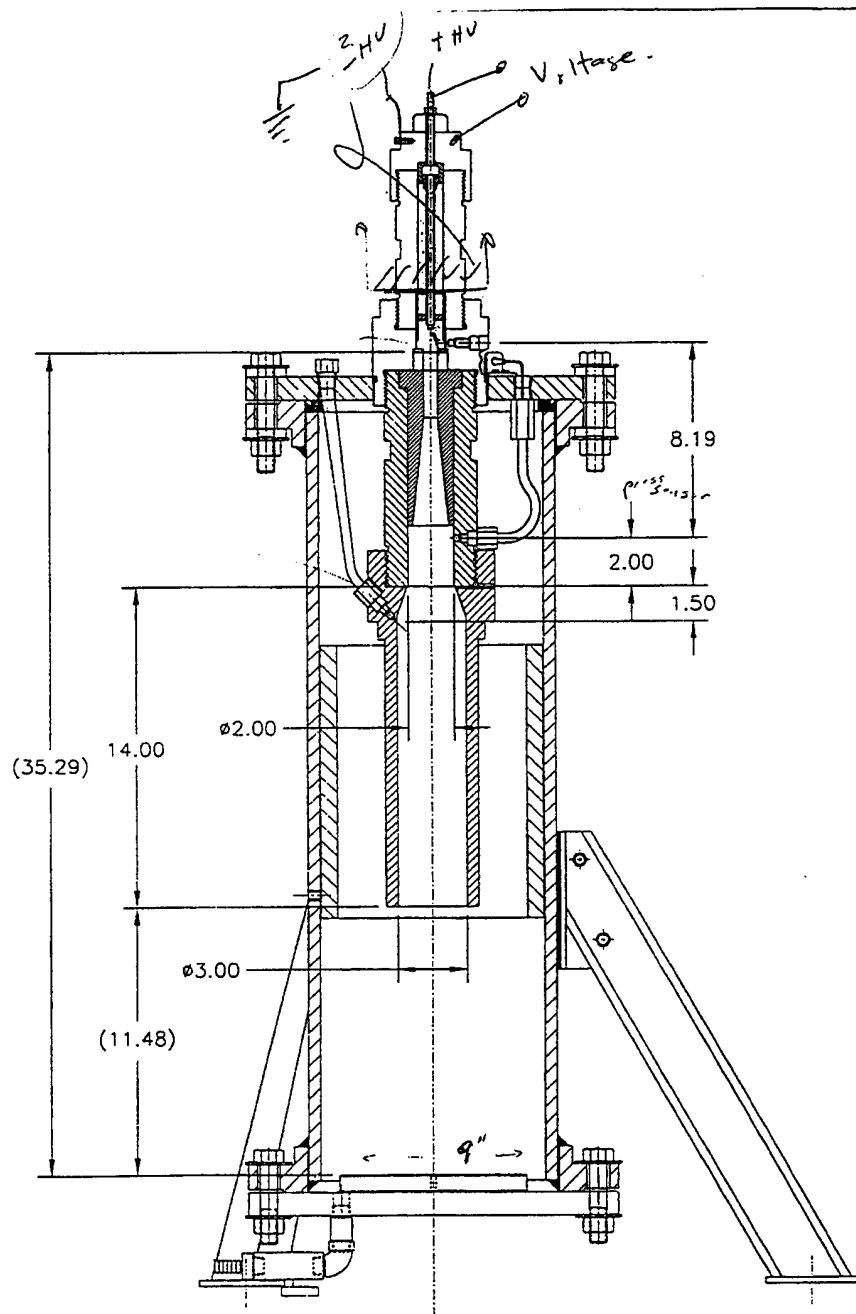
Figure 5.2 – Test apparatus for Phase One testing.
Pressure sensors are located within the combustion chamber,
nozzle assembly and base of the extender tube.

The drawing title block reads:

ITEM	QTY.	DWG NO.	DESCRIPTION
7	4		EYE BOLT 1/2-13UNC
6	18	91251A712	SCREW, SCH,1/2-13UNC-3A X1.0
5			
4	2	10543	BRACE, STRAP, PRIMARY DIST., 4X
3	2	10542	BRACE, SUPPORT PRIM DIST., 4X
2	2	10541	BRACE, BASE, PRIMARY DIST., 4X4
1	2	10536	PLATE, SOURCE, MOUNTING, 4X4

UNLESS OTHERWISE SPECIFIED
DIMENSIONS ARE IN INCHES.
TOLERANCES:
.XX: ± .25
.XXX: ± .125
∢: ± 1°
x/x: ± 1/16
SURFACE: √ 125

MATERIAL:
UNLESS OTHERWISE SPECIFIED
PURCHASED PARTS ARE
McMASTER-CARR PART NO'S

ADVANCED POWER TECHNOLOGIES, IN
1250 24th ST. NW, SUITE 850
WASHINGTON, DC 20037

HOUSING,
SOURCE, 4X4

SIZE A   SCALE: 1/8   DWG NO. 1030.
BY: PJL   05/22/00   SHEET: 1 OF

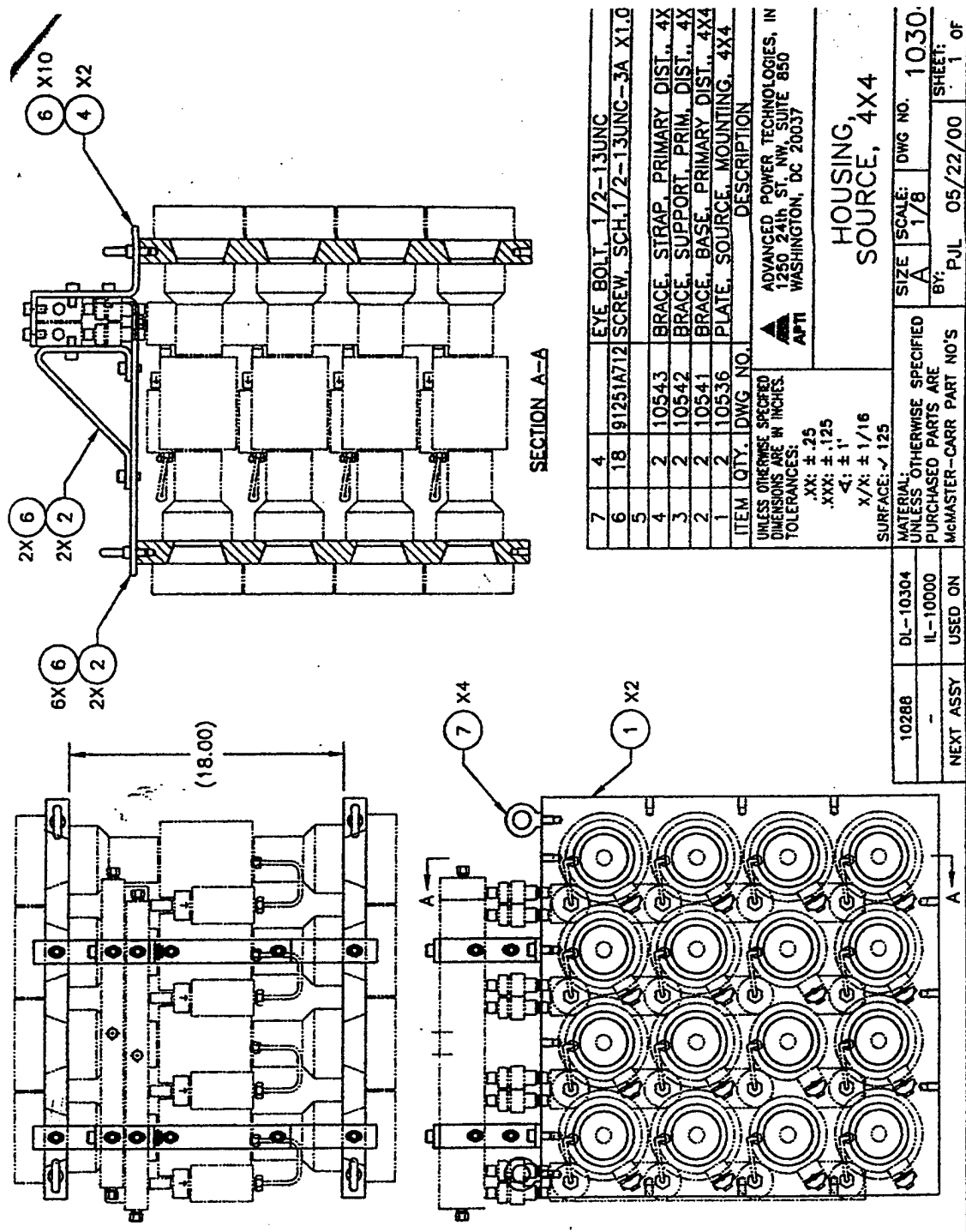| 10288	DL-10304	IL-10000	
NEXT ASSY	–	USED ON	

SECTION A-A

(18.00)

Figure 5.3 – Phase Three testing apparatus consisting of 16
double-ended nozzles.

system, an opposed nozzle system was utilized. In this manner, the associated shock wave emitting from the nozzles opposed one another and thus cancels out any sidereal forces acting on the device. As a result, Waterhammer remained stationary for the entire test process. This portion of the testing was conducted at Briar Point Underwater Test Range in Aberdeen Proving Grounds, Aberdeen, MD. Waterhammer was suspended from a large floatation device 17 ft below the surface, depicted in Figure 5.4. Although located on a slope, the depth of the water at that location measured approximately 35 ft. The exact location of the device in relation to the bottom topography is shown in Figure 5.5. To characterize the pressure field and beam patterns associated with each firing, pressure sensors were placed in locations depicted by Figures 5.6 and 5.7.
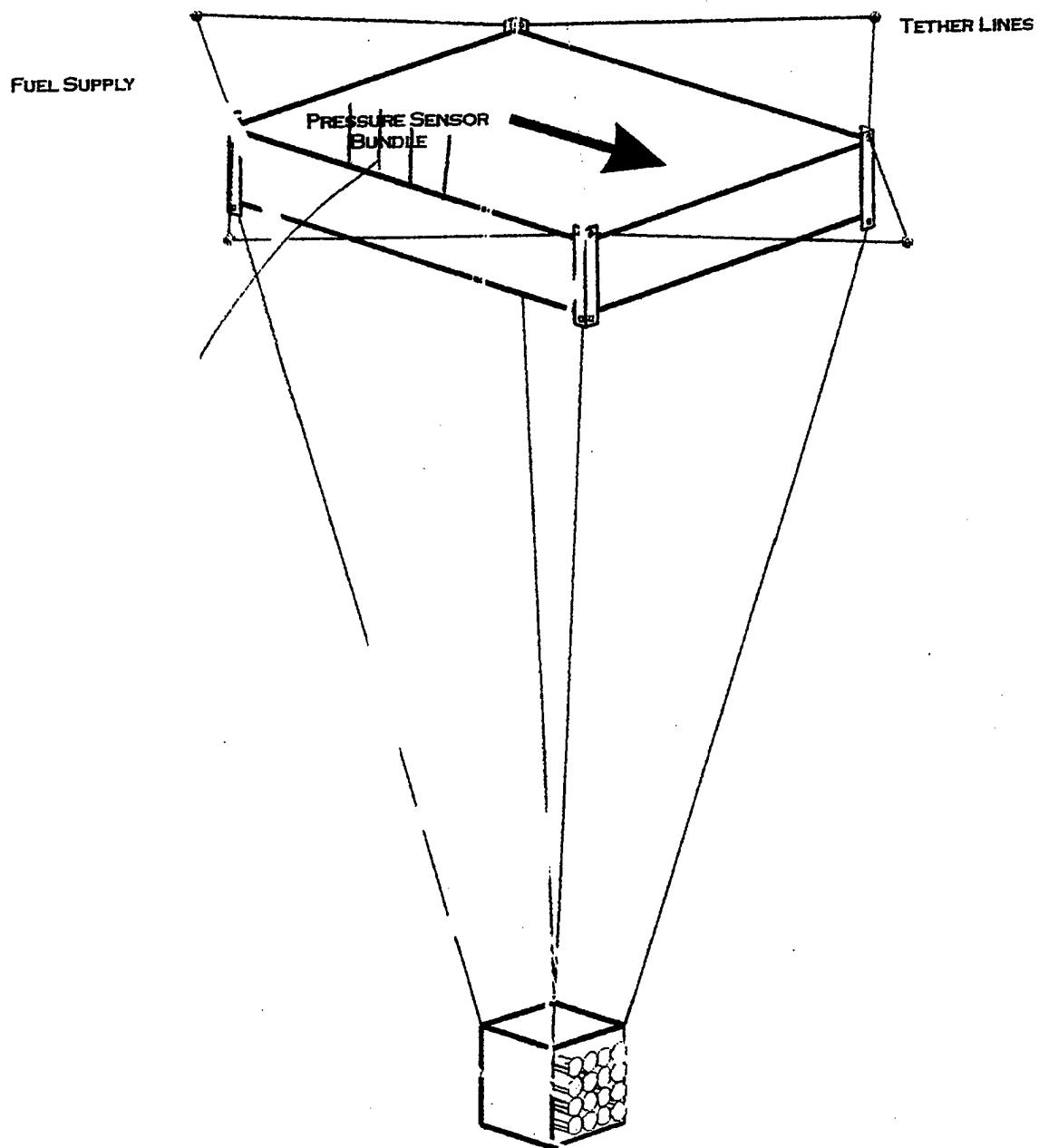
Figure 5.4 – Graphical depiction of floatation device used
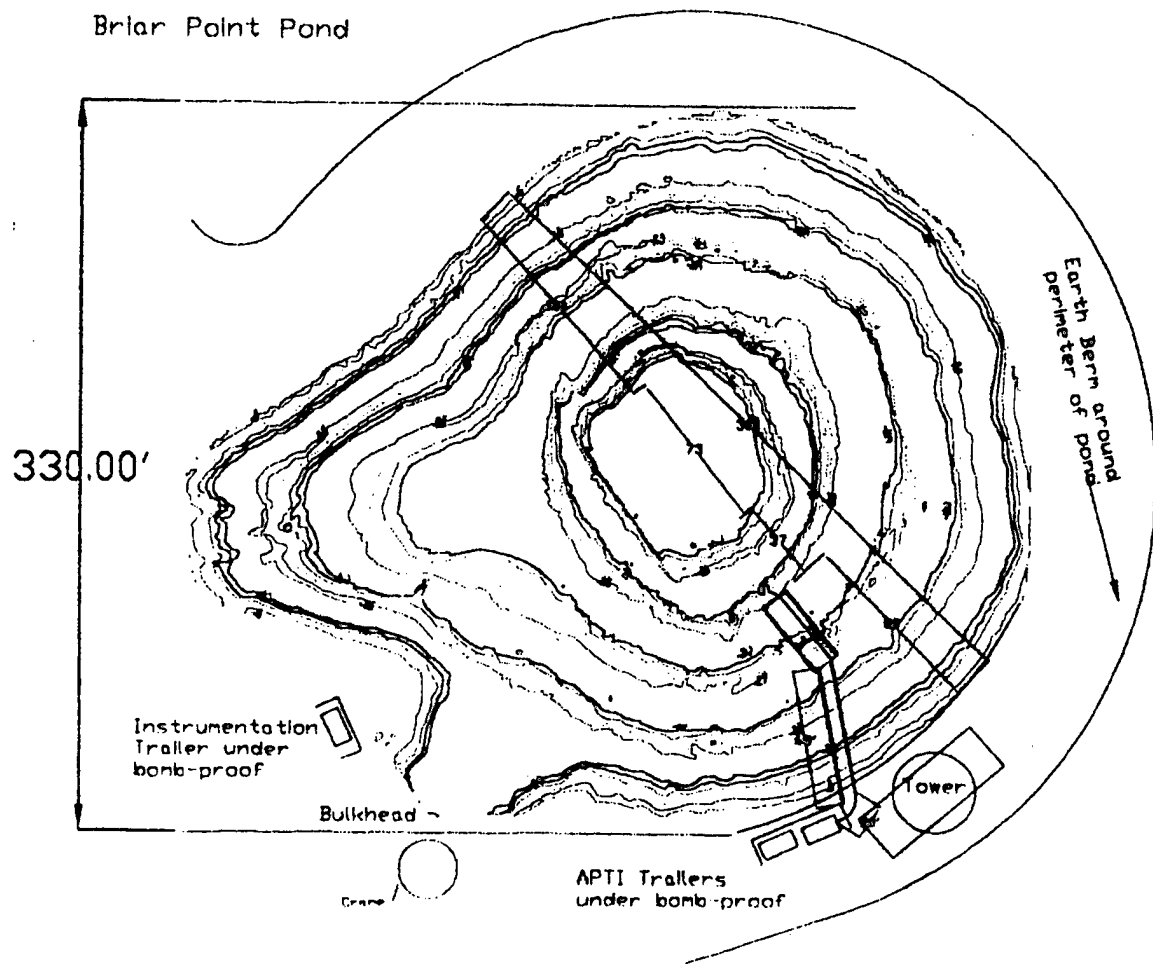to suspend Waterhammer 17 feet below the surface.

Figure 5.5 – Bottom topography chart of Briar Point
Underwater Range at Aberdeen Proving Grounds, Aberdeen, MD,
with testing infrastructure overlaid.
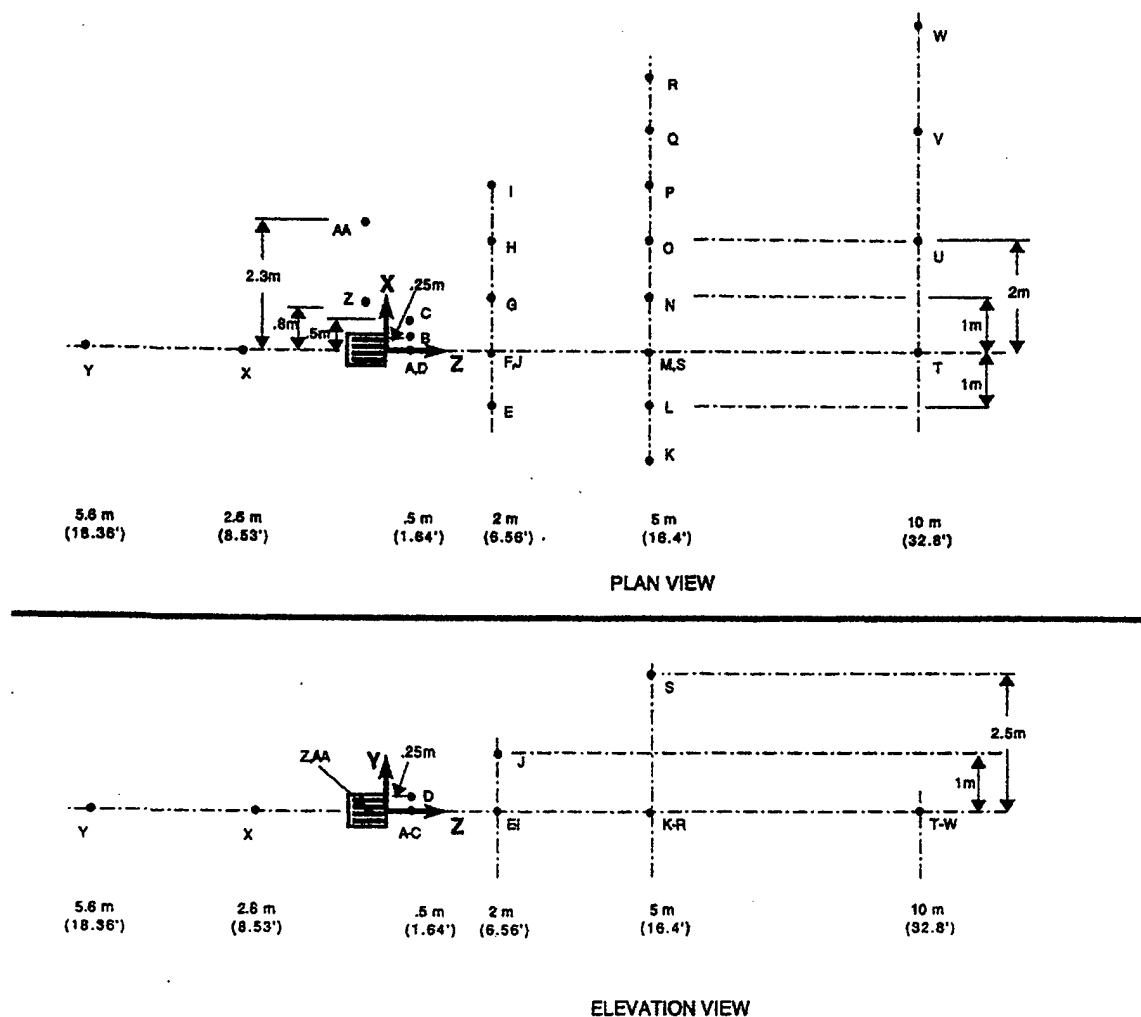
PLAN VIEW

ELEVATION VIEW

Figure 5.6 – Pressure sensor locations during phase three testing. Top illustration is a plan, or Birdseye view of sensors, while bottom portion of figure indicates sensor elevation in relation to the center of Waterhammer.
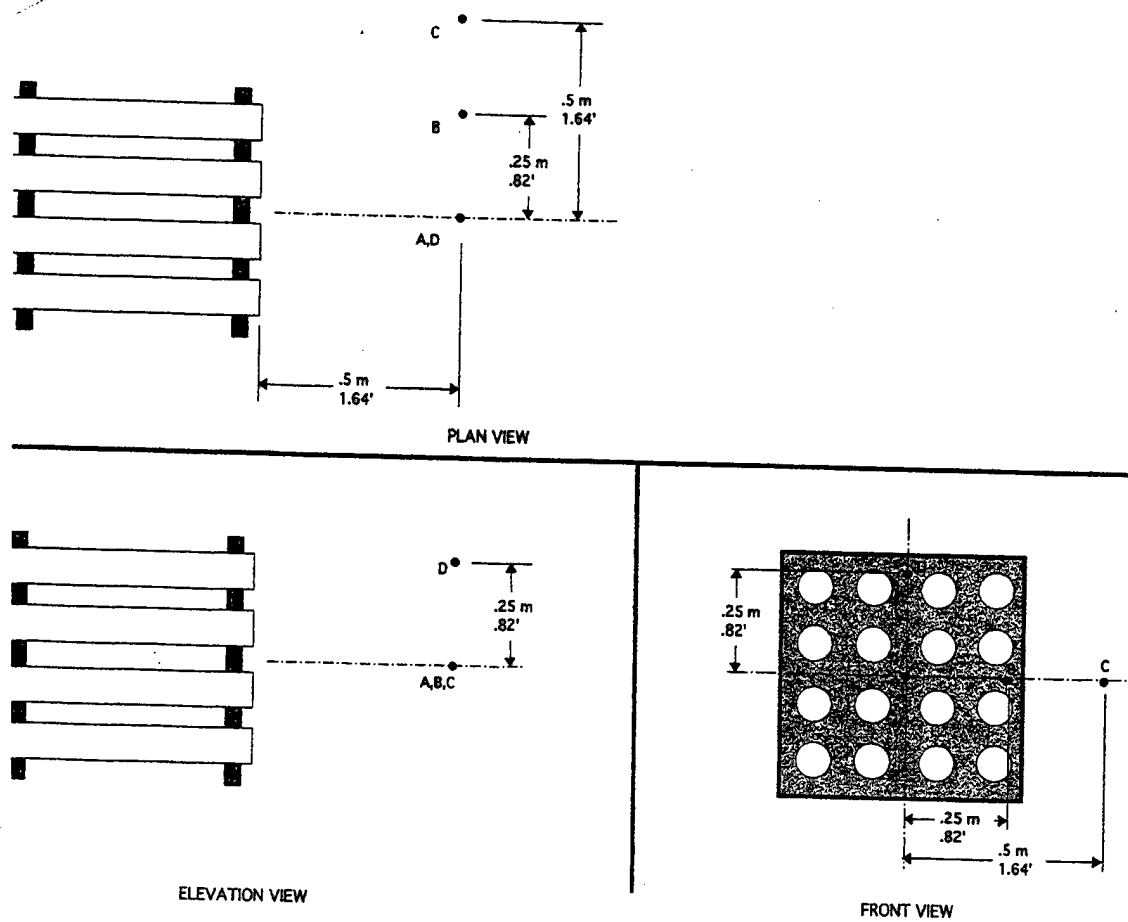
33

PLAN VIEW

ELEVATION VIEW

FRONT VIEW

Figure 5.7 - Magnified view of sensors located close to
Waterhammer during phase three testing.

VI. CALCULATIONS AND RESULTS

A. GENERAL PARAMETERS

In order for the shock wave to completely envelop a mine it has been determined that a pulse length of 450 μsec is required, corresponding to a frequency of roughly 2.22 khz or $\omega = 2\pi f = 13.96 \times 10^3$. The sound speed within fresh water is $c_0 = 1480$, while in seawater $c_0 = 1500$.

B. TRANSMISSION LOSS

As the deflagration occurs within Waterhammer, the resulting shock wave is propagated into the medium. The resulting energy is then spread equally throughout the water in multiple paths, or modes, until it reaches its target. The number of modes present can be calculated as (Ref. 6)

$$(m - \tfrac{1}{2})\pi/D \leq \omega/c$$

The number of mode present is indicated by m and D is the depth of the medium. With the knowledge that $\omega = 2\pi f$ and solving the above formula for the amount of modes present results in:

$$m \leq 2fD/c + \tfrac{1}{2}$$

Using a depth of 12.2 meters, corresponding to the deepest water the device was intended to be used, results

in 36 modes propagating. As the depth decreases, so will the amount of propagating modes. At a depth of 1 meter, the lowest end of the expected operating range, only three modes will propagate. Using a bottom profile chart of the Briar Point underwater range at Aberdeen Proving Grounds, and a simple Parabolic Equation (PE) model, transmission loss predictions were generated for Waterhammer phase three testing. The PE model calculates transmission losses in relation to range and depth. Bottom and surface effects, which affect the amount of propagating modes, are included in the model through the use of Split-Step Fourier (SSF) analysis (Ref. 7). Basic assumptions are required for this model to accurately predict the transmission loss results. These assumptions include the bottom composition to be uniform and fast (c = 1730 m/s), the bottom type extends down beyond 22 meters of depth, and the slope of the bottom to be of a constant value. Briar Point's bottom composition consisted of quartz and coarse sand, indicative of a fast bottom. For this model, the bottom composition was considered to contain a uniform distribution of quartz and coarse sand down to a depth of 22 meters below the surface. Layers of mud or air pockets beneath the initial quartz and course sand interface would create errors within

the propagating modes. Applying SSF analysis within the PE

model results in the Transmission Loss graph shown in

Figure 6.1. Each blue 'X' represents the location of a

pressure sensor during phase three testing. For test

firing number 5005 conducted on 24 Jul 2000, the source

level corresponded to roughly 265 dB (relative to 1 μPa) at

the radiating face. After applying the Source Level (SL)

of 265 dB to the Transmission Loss predictions results in

received pressure levels at various depths over the range

of the pond. Figure 6.2 displays these results in dB

relative to 1 μPa. From Figures 6.1 and 6.2, it becomes

readily apparent that energy is distributed equally across

all modes. As these modes propagate independently through

the region of interest, magnitudes and phases are combined

together to resulting in regions of constructive and

destructive interference. Also included in this model is

the attenuation of sound into the bottom. The quartz and

coarse sand bottom absorbs sound and energy with each modes

impact, providing the impact angle is less than the

critical angle. At angles of impact greater than the

critical angle the energy is reflected back into the water

column. These figures also depict a great deal of energy

that is transmitted into the bottom, where it continues to

propagate downward, effectively stealing the energy from the water column. Figure 6.3 shows predicted results for each sensor location as compared to the actual test data. Although minor discrepancies occur, predicted values correlate well with test data, validating the model and the SSF process. These minor discrepancies result from a non-uniform bottom and a nonlinear slope that were used as basic assumptions in the model.

The SSF model is only designed to operate with sources operating well below the saturation limit, where the nonlinear effects of water are not present. This model was used for the phase three testing because of the relatively low source level used for testing. As the source level is increased and nonlinear effects become more apparent, this model will begin to break down.
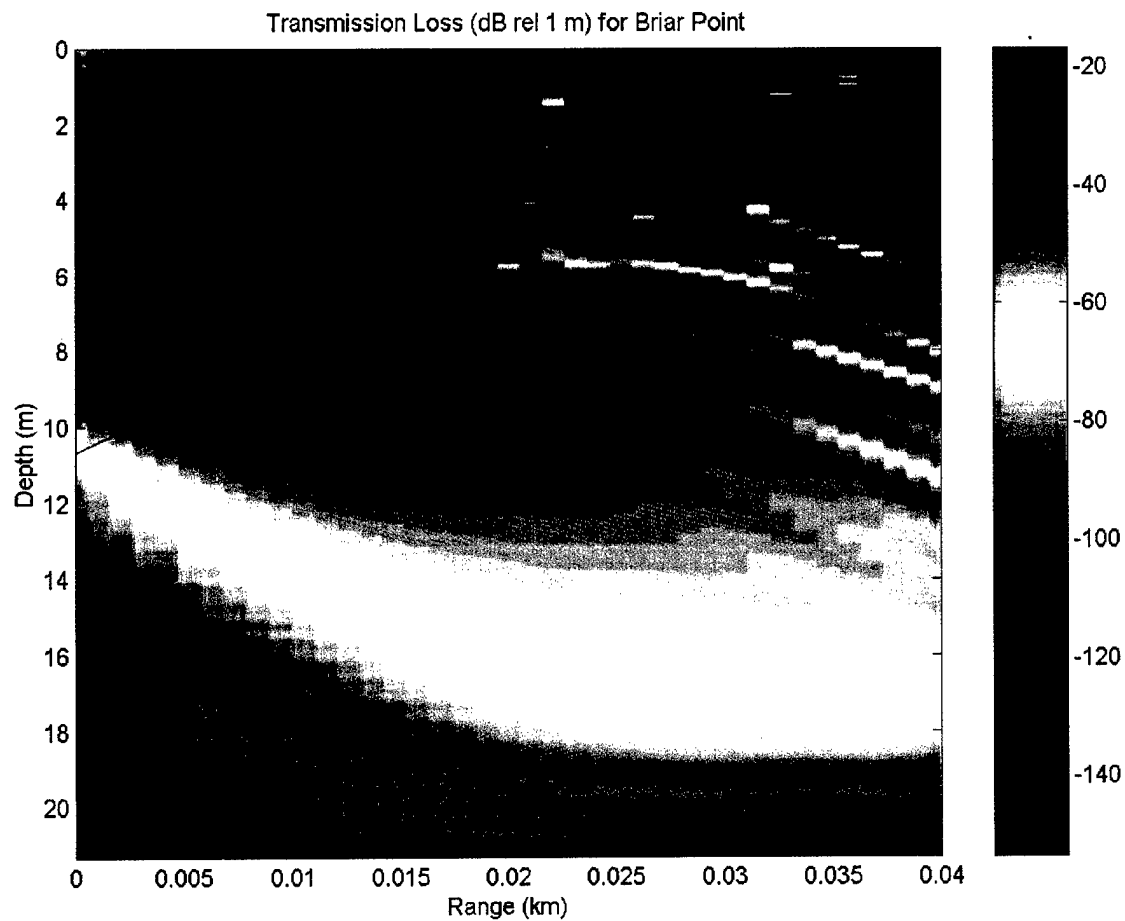
Figure 6.1 - Transmission Loss calculations for the Briar
Point Underwater Range at Aberdeen Proving Grounds in
Aberdeen, MD.

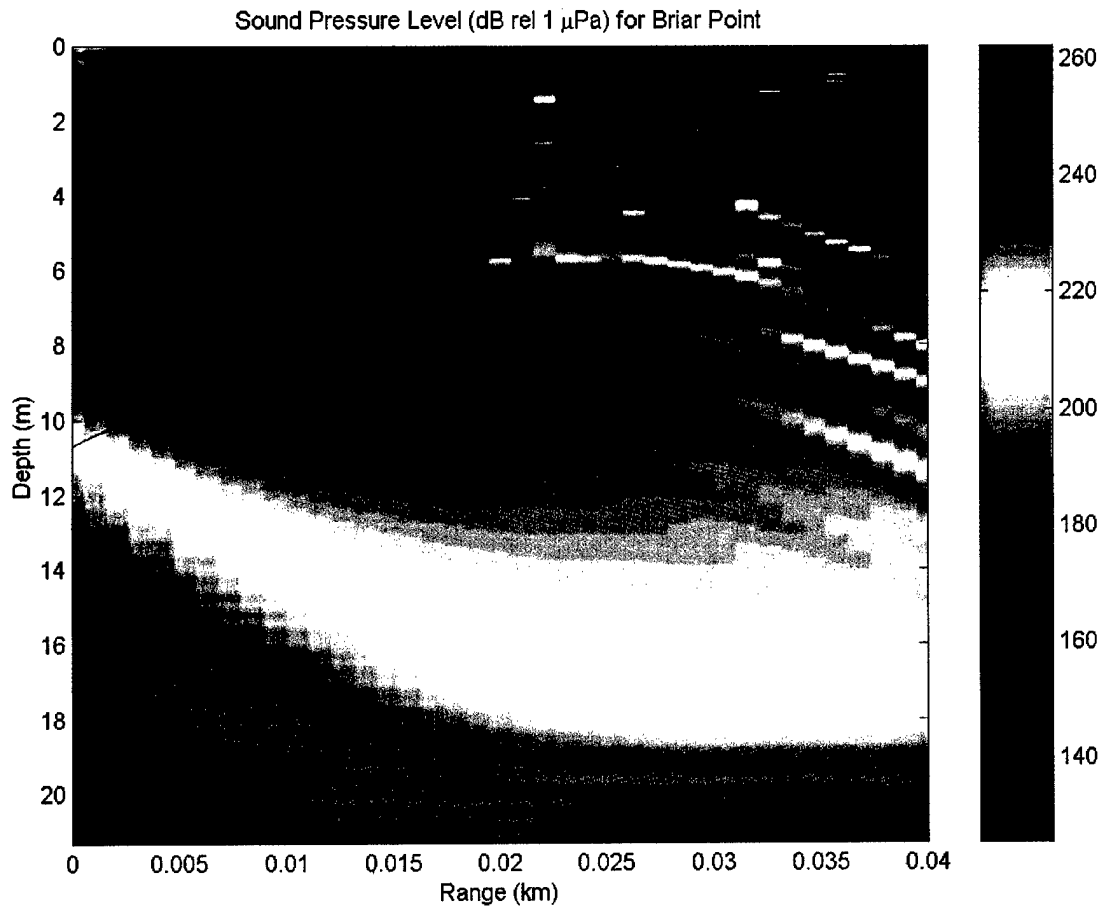Sound Pressure Level (dB rel 1 μPa) for Briar Point

Figure 6.2 - Received pressure calculations for the Briar
Point Underwater Range at Aberdeen Proving Grounds in
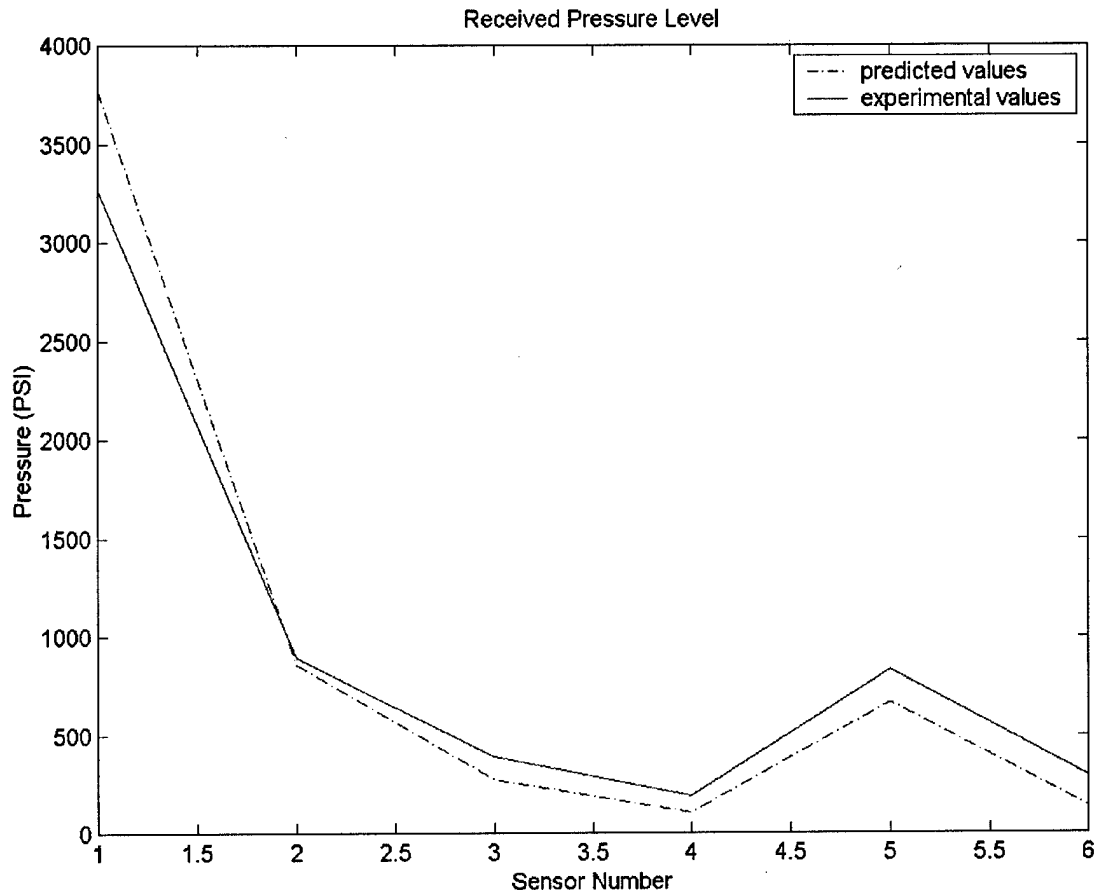Aberdeen, MD.

Figure 6.3 - Predicted vs. Experimental data for phase three testing at Briar Point Underwater Range at Aberdeen Proving Grounds in Aberdeen, MD. Predicted values appear as a black dashed line while experimental data is depicted as a solid blue line.

C. SATURATION EFFECTS

As the pressures are increased and nonlinearities become more important, Waterhammer will be limited to the saturation curves for the medium in which it is immersed. Using the equations provided from Chapters III and IV, Figure 6.4 is produced. From this figure, it becomes

obvious that the shock wave pressures rapidly diminish with range. From empirical calculations, an impulse of 1000 psi·μsec is desired for an effective means of disposing mines and obstructions. Re-plotting Figure 6.4 in a different scale and applying the desired benchmark yields Figure 6.5. From this graph it is apparent that Waterhammer will have a lethal range of 5.81 yards.
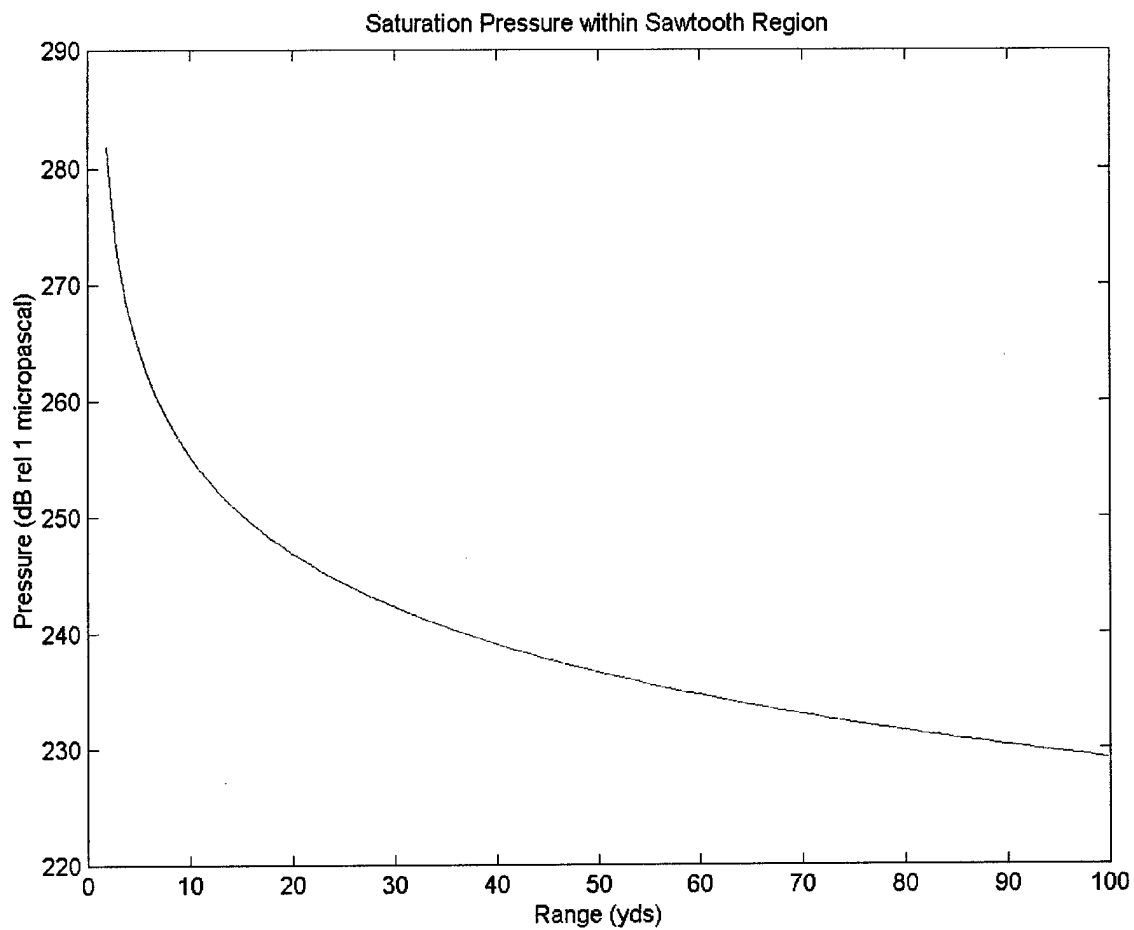
Figure 6.4 - Saturation curve depicted as a function of Pressure in dB rel 1μPa over distances within the sawtooth region.
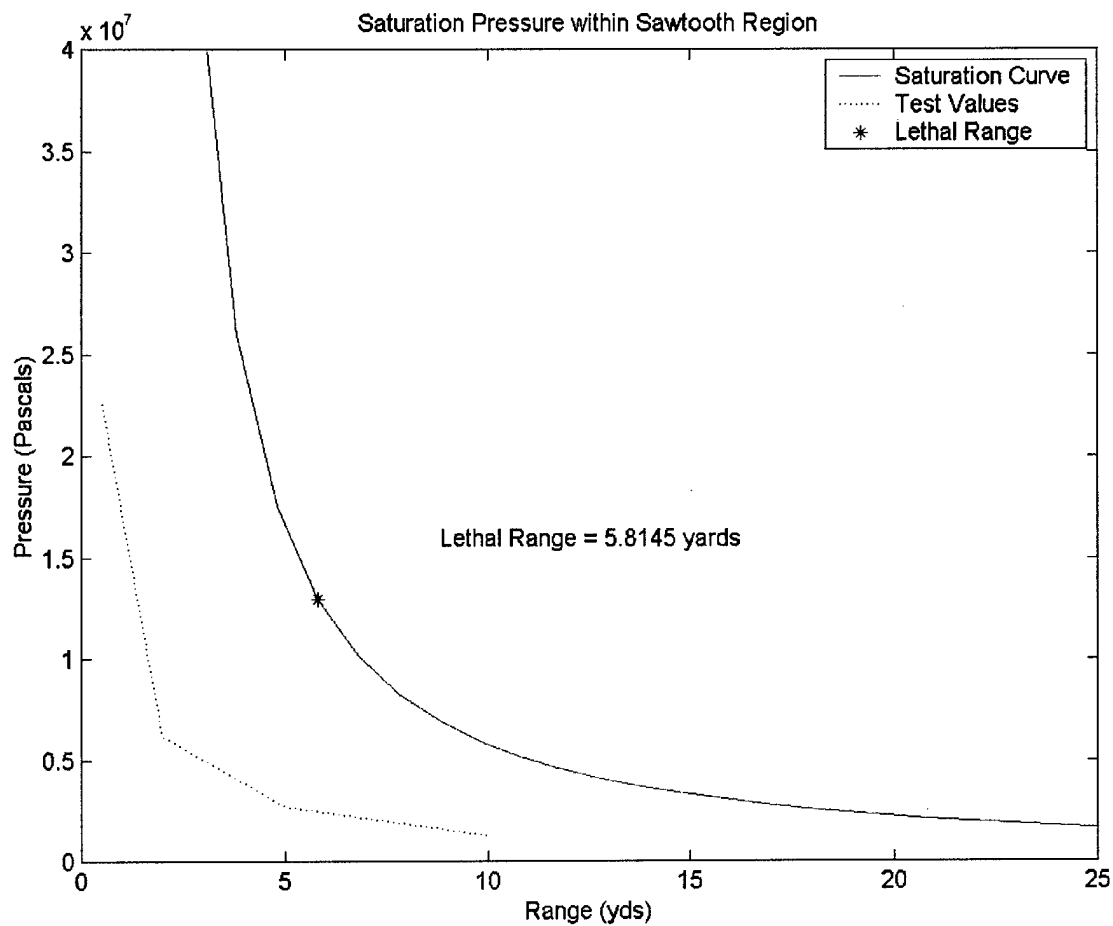
Figure 6.5 - The same saturation curve as Figure 6.4 redrawn for pressure in Pa (red solid line), including test data (black dashed line) and lethal range calculations (asterisk) based on a 1000 psi·μsec impulse.

VII. CONCLUSION

In the view of this thesis, nonlinear effects quickly become a significant factor in the effectiveness of Waterhammer. The theory basis for this thesis and the agreement between predicted and observed pressure levels (Fig 6.3 and 6.5) appear to indicate a lethal range of only 5.81 yards for Waterhammer, even if the source amplitude is increased significantly. At these short ranges, surface and bottom reflections as well as bottom propagation (Fig 6.2), that would otherwise reduce the acoustic energy density intended for lethality, may not play any role. The reduced ranges indicate that many units will be required to work cooperatively in order to effectively clear a usable path to the beach. Unfortunately, with effective ranges of this magnitude, the size of each device and the logistics of placing enough devices in theater appear to significantly reduce the viability of Waterhammer as a solution to the mine clearance problem in the very shallow water region.

The concept for using shock waves to clear a path to the beach is revolutionary and creative and it may still remain applicable in the mine warfare arena. However the results of this thesis suggest that Waterhammer in its current concept should be amended.

LIST OF REFERENCES

1. Naval Mine Warfare Engineering Activity, *NAVSEA Mine Familiarizer*, United States Navy, 1985.

2. Urick, R. J., *Principles of Underwater Sound Third Edition*, McGraw-Hill, Inc., 1983.

3. Cooper, P. W. and Kurowski, S. R., *Introduction to the Technology of Explosives*, Wiley – VCH, Jan 1997.

4. Larraza, A., *Nonlinear Acoustics Class Notes*

5. Shooter, J. A., Muir, T. G., and Blackstock D. T., "Acoustic saturation of spherical waves in water", *The Journal of the Acoustical Society of America*, vol. 55, no. 1, pp 54-62, Jan 1974.

6. Kinsler, L. E., Frey, A. R., Coppens, A. B., Sanders, J. V., *Fundamentals of Acoustics Fourth Edition*, John Wiley & Sons, Inc., 2000.

7. Hardin, R. H. and Tappert, F. D., *Applications of the split-step Fourier method to the numerical solution of nonlinear and variable coefficient wave equations*, SIAM Rev. 15, pp. 423, 1973.

THIS PAGE INTENTIONALLY LEFT BLANK

INITIAL DISTRIBUTION LIST

1. Defense Technical Information Center 2
    8725 John J. Kingman Road, Suite 0944
    Ft. Belvoir, VA 22060-6218

2. Dudley Knox Library 2
    Naval Postgraduate School
    411 Dyer Road
    Monterey, CA 93943-5101

3. Andres Larraza 1
    Naval Postgraduate School
    589 Dyer Road, Room 110 (Code PH)
    Monterey, CA 93943

4. John D. Pearson RADM, USN (ret) 1
    Naval Postgraduate School
    589 Dyer Road, Room 205B (Code UW)
    Monterey, CA 93943

5. Mark Machina 1
    APTI
    1400 A Duke St.
    Alexandria, VA 22314

6. Dr. Frank Shoup 2
    Associate Director, Expeditionary Warfare Div. (N85T)
    Office of the Chief of Naval Operations
    2000 Navy Pentagon 4A720
    Washington, DC 20350-2600

7. Dr. Doug Todoroff 2
    Office of Naval Research
    Code 322W
    800 N. Quincy St.
    Arlington, VA 22217-5660

8. Ronald J Karun LT, USN 2
    1408 Buffalo St.
    Peru, IL 61354